

Studies on the thermal decomposition of basic lead(II) carbonate by Fourier-transform Raman spectroscopy, X-ray diffraction and thermal analysis†

Dan A. Ciomartan,^a Robin J. H. Clark,^a Lachlan J. McDonald^a and Marianne Odlyha^b

^a Christopher Ingold Laboratories, University College London, 20 Gordon Street, London WC1H 0AJ, UK

^b Department of Chemistry, Birkbeck College, Gordon House, 29 Gordon Square, London WC1H 0AJ, UK

The thermal decomposition of basic lead(II) carbonate $2\text{PbCO}_3 \cdot \text{Pb}(\text{OH})_2$ in static air under atmospheric conditions has been studied for the first time using a combination of thermoanalytical, X-ray diffraction and Raman spectroscopic techniques. New intermediate compounds of the type $4\text{PbCO}_3 \cdot 3\text{PbO}$ and PbCO_3 have been observed in addition to previously reported ones of the type $2\text{PbCO}_3 \cdot \text{PbO}$, $\text{PbCO}_3 \cdot \text{PbO}$ and $\text{PbCO}_3 \cdot 2\text{PbO}$. Post-decomposition studies have identified the presence of the tetragonal-to-orthorhombic phase transition in PbO . Results are also presented for the decomposition processes in nitrogen and oxygen atmospheres. Oxidative decomposition studies have shown that Pb_3O_4 forms in oxygen and in flowing air.

Basic lead(II) carbonate, $2\text{PbCO}_3 \cdot \text{Pb}(\text{OH})_2$, also known as flake white, lead white, and white lead, occurs naturally as the rare mineral hydrocerussite.¹ It is one of the oldest synthetic pigments (*ca.* 300 B.C.) and is a fine compact, shiny white material² which is known to be unstable in the presence of certain reagents, notably H_2S .^{3,4} The ancient methods of preparation are not well understood, the raw materials being either sheets of metallic lead or various lead oxides such as PbO , Pb_3O_4 , together with vinegar.^{5–7} Many patents have been registered as variants on the six main methods for its preparation, leading to products of various compositions $x\text{PbCO}_3 \cdot \text{Pb}(\text{OH})_2$, where x varies from 1.8 to 3.6.⁸ Due to this variation in its stoichiometry with preparative procedure, only an approximate structure⁹ for basic lead(II) carbonate could be determined by Cowley¹⁰ using electron diffraction on a powdered sample. Later Olby¹¹ showed that Cowley had actually determined the structure of a related compound plumbonacrite, $\text{Pb}_{10}(\text{CO}_3)_6(\text{OH})_6\text{O}$ and not that of hydrocerussite $2\text{PbCO}_3 \cdot \text{Pb}(\text{OH})_2$. The X-ray powder diffractograms of both of these compounds and of PbCO_3 have been given;^{11,12} the structure of PbCO_3 (cerussite) has also been determined by X-ray diffraction⁹ and later refined by neutron diffraction.¹³

Good quality Raman and Fourier-transform (FT) Raman spectra of powdered PbCO_3 have been obtained and six of the main bands assigned.^{14–17} The presence of white lead of unspecified stoichiometry, $x\text{PbCO}_3 \cdot \text{Pb}(\text{OH})_2$, has been identified on illuminated manuscripts by Raman microscopy.^{18,19}

The thermal decomposition of PbCO_3 (cerussite) has been studied in considerable detail by a number of workers.^{20–23} The decomposition process is complex and involves several stages with the formation of lead carbonate oxides. Studies have also been performed on both natural and synthetic forms of $2\text{PbCO}_3 \cdot \text{Pb}(\text{OH})_2$ (hydrocerussite).²² Initially loss of hydroxyl water occurs and this is followed by the formation of intermediate carbonate oxides. The temperature range of the decomposition process as measured in these studies is 508–823 K.

Additional studies of PbCO_3 ²⁴ and $2\text{PbCO}_3 \cdot \text{Pb}(\text{OH})_2$ ²⁵ in CO_2 at atmospheric pressure, involving thermogravimetric analysis (TGA), differential thermal analysis (DTA), X-ray

diffraction (XRD) and infrared spectroscopy (IR), have shown that three solid intermediates, $2\text{PbCO}_3 \cdot \text{PbO}$, $\text{PbCO}_3 \cdot \text{PbO}$ and $\text{PbCO}_3 \cdot 2\text{PbO}$, are formed between 373 and 773 K. The same intermediate products have been isolated²⁶ from the thermal decomposition of PbCO_3 ²⁴ by heating stoichiometric mixtures of PbO and PbCO_3 in CO_2 until equilibrium was reached. The products obtained were characterised by X-ray diffraction. A new lead(II) carbonate oxide $4\text{PbCO}_3 \cdot 3\text{PbO}$ was reported, in addition to those reported to be formed at high pressures.^{24,25} The thermal decomposition of $2\text{PbCO}_3 \cdot \text{Pb}(\text{OH})_2$ ²⁷ and PbCO_3 ²⁸ has been studied by analysis of the variation of electrical resistance as a function of temperature at various pressures and some of the intermediate products, such as plumbonacrite,¹¹ yellow PbO , and metallic Pb , have been characterised by XRD.

The aim in this paper was to study the thermal decomposition of $2\text{PbCO}_3 \cdot \text{Pb}(\text{OH})_2$ in static air using a combination of thermal techniques (TGA and differential scanning calorimetry, DSC), FT Raman spectroscopy, and XRD in order to understand the mechanism of the decomposition process and to characterise the intermediate compounds. It was also of interest to identify the transition in PbO from tetragonal to orthorhombic (the mineral massicotite²⁹ is orthorhombic PbO). The crystal structures of both tetragonal and orthorhombic PbO have been determined by X-ray and neutron diffraction,^{30–34} and the powder X-ray diffractograms of both tetragonal and orthorhombic PbO have been given.^{12,35} Other studies include those on the polymorphism of PbO at high pressures and temperatures,³⁶ the spontaneous transformation at room temperature of a single crystal of orthorhombic PbO to tetragonal,³⁷ the bonding in the two forms of PbO ,^{38,39} and the vibrational spectra as powders⁴⁰ and single crystals.⁴¹ Raman and FT Raman spectra of PbO and Pb_3O_4 have been reported for the region above 100 cm^{-1} .^{42,43}

A further aim was to compare the effect of different atmospheres, inert and reactive, on the decomposition process. The information could assist in understanding how Pb_3O_4 had been obtained in the past from the roasting of white lead.⁴⁴

Experimental

Materials

Basic lead(II) carbonate (Aldrich) was selected for all experiments, since it is stable and has the well known

† Supplementary data available (No. SUP 57161, 4 pp.): Fourier-transform Raman spectral data. See Instructions for Authors, *J. Chem. Soc., Dalton Trans.*, 1996, Issue 1.

stoichiometry $2\text{PbCO}_3 \cdot \text{Pb}(\text{OH})_2$ in preference to the commercial product sold as a white lead.^{3,8} Lead carbonate PbCO_3 and red lead Pb_3O_4 , both also from Aldrich, were used as reference materials.

Thermal analysis

The TGA/DTGA curves in static air as well as in flowing air, in O_2 and in N_2 ($20 \text{ cm}^3 \text{ min}^{-1}$) were obtained using a Shimadzu TG-50 thermoanalyser at a heating rate of 2 K min^{-1} . The corresponding DSC curves were obtained using a Shimadzu DSC-50 differential scanning calorimeter at the same heating rate and in the same atmosphere. Samples of ca. 20 mg were heated in both aluminium and alumina crucibles for both DSC and TGA studies.

Preparation of samples for FT Raman and XRD analysis

From a preliminary thermogravimetric curve which showed the decomposition of $2\text{PbCO}_3 \cdot \text{Pb}(\text{OH})_2$ in static air, 22 temperatures were selected encompassing all of the observed thermal phenomena (Fig. 1). Samples (0.5 g) of basic lead(II) carbonate in alumina boats (Degussa Ltd.) were heated individually in a tube furnace in static air at the preselected temperature ($\pm 5 \text{ K}$) for 6 min, and then quenched at room temperature on a metallic plate. The sample temperature was measured with a precision of $\pm 1 \text{ K}$ in the furnace near the centre of the alumina boat with a thermocouple type K (NiCr/NiAl) attached to a Comark instrument. Quenched samples were ground in an agate mortar, but not finely, in order to preserve the structure of the high-temperature phases (especially those of samples containing lead oxides). Such structures may be modified on being ground.⁴⁵⁻⁴⁷

Red lead, Pb_3O_4 , was obtained by heating $2\text{PbCO}_3 \cdot \text{Pb}(\text{OH})_2$ in oxygen to 838 K in the TGA equipment, and the yellow-orange sample of PbO by heating in the same way in nitrogen to 648 K.

FT Raman spectroscopy

The FT Raman spectra between 50 and 3600 cm^{-1} were obtained using a Nicolet Raman spectrometer (FT Raman 910), having a Nd/YAG laser (1064 nm excitation) and a germanium detector cooled at liquid-nitrogen temperature. The spectrometer was calibrated using the spectral lines of a neon lamp. Corrections for the instrument response and for the wavenumber of the Rayleigh line (ICR and ARS macros) were applied to all FT Raman spectra unless otherwise specified. The wavenumbers are accurate to $\pm (1-2) \text{ cm}^{-1}$.

X-Ray diffraction

X-Ray diffractograms between 5 and 65° (2θ) were collected in steps of 0.04° (2θ) at an integration time of 1 s using $\text{Cu-K}\alpha_1$ radiation at $\lambda = 0.15406 \text{ nm}$, monochromatised by a germanium single crystal, on a Siemens diffractometer (D-5000). Noise and background corrections were applied to all of

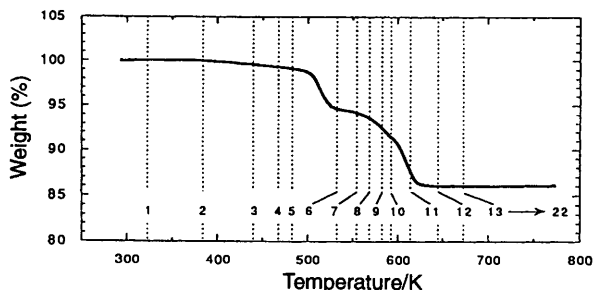


Fig. 1 The TGA curve for thermal decomposition of basic lead carbonate in static air in an aluminium crucible showing the temperatures selected for FT-Raman and X-ray diffraction studies of the compounds prepared

the diffractograms. The crystalline structures of each of the samples were identified using the EVA programme from the package DIFRAC AT V3.2 supplied by Siemens. The 'Figure of Merit' (FOM) is a criterion of selection of a phase in a search-match procedure using JCPDS files: FOM = 0 for an ideal selected phase whose lines match exactly with those given by the appropriate JCPDS file. All phases with FOM > 2 were rejected.

Results and Discussion

Decomposition of $2\text{PbCO}_3 \cdot \text{Pb}(\text{OH})_2$ in static air

Thermal analysis. The decomposition of basic lead(II) carbonate was studied by thermogravimetry in static air. The weight loss showed two main steps which may conceal further processes [see Fig. 2(a)] as is more clearly indicated by the first derivative of the TGA curve (DTGA). From the DSC curve [Fig. 2(b)] there seem to be two endothermic processes which are correlated with the main decomposition steps; between these is an exothermic process which may be an indication of the formation of intermediate carbonate oxide compounds still to be characterised. This is followed by a broad endothermic peak in the appropriate range 635–750 K which is not accompanied by any change in the mass of the sample and a phase change is implied.

FT Raman spectroscopy. All the Raman bands detected in the spectra of samples 1–22, together with those of PbCO_3 and Pb_3O_4 , are listed in SUP 57161.

The spectra of samples 1–5 in Fig. 3(a) show that there is no structural change in $2\text{PbCO}_3 \cdot \text{Pb}(\text{OH})_2$ between 322 and 483 K. Detailed spectra of samples 1 and 5 are given in Fig. 4(a) and 4(b). In Fig. 4(c) the spectrum of an unheated sample of PbCO_3 is given, to be compared with the spectrum of sample 6 [Fig. 4(d)] which forms at 533 K. It is suggested that in sample 6 all of the OH^- groups have been ejected from the molecule as

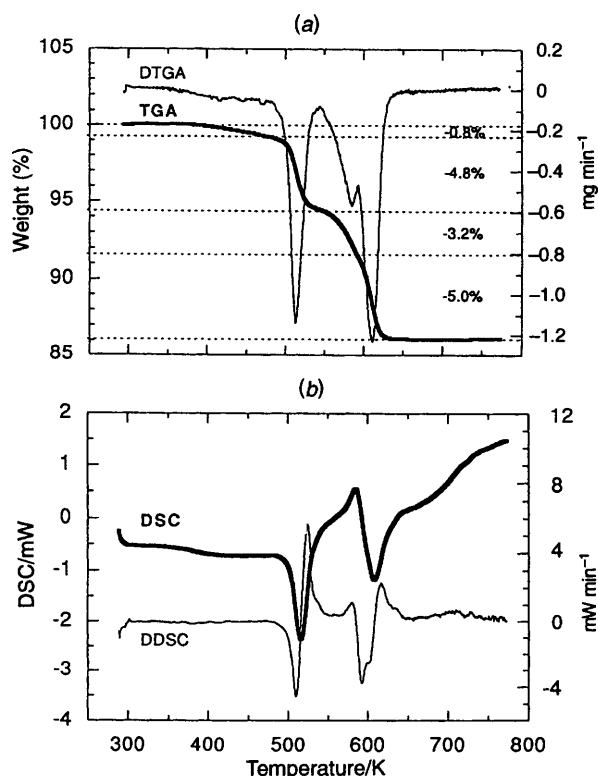


Fig. 2 (a) The TGA and DTGA curves for the thermal decomposition of basic lead carbonate in static air in an aluminium crucible showing the progressive weight losses. (b) The corresponding DSC (and first derivative) curves

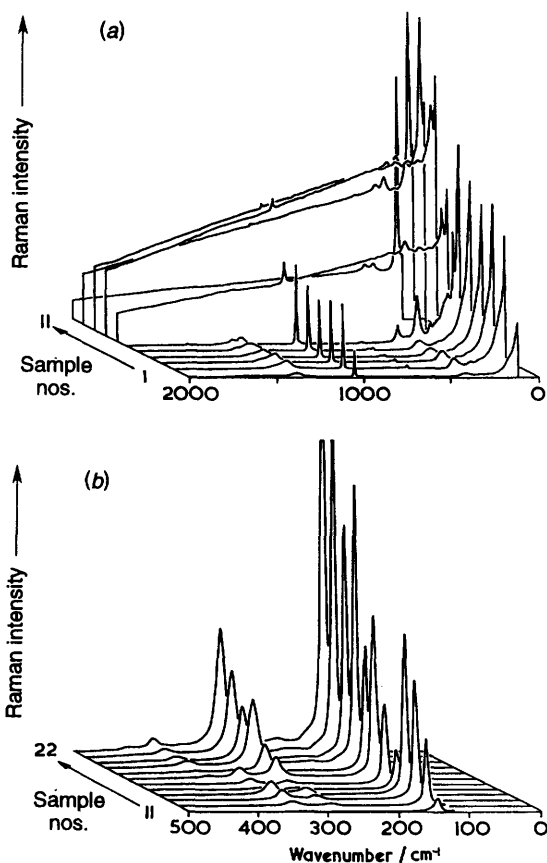


Fig. 3 The FT Raman spectra of the 22 samples of $2\text{PbCO}_3 \cdot \text{Pb(OH)}_2$ after having been heated in a tube furnace in static air at increasing temperatures and quenched to room temperature: (a) samples 1–11 (322–613 K); (b) samples 11–22 (613–898 K)

water. The broad band at *ca.* 1365 cm^{-1} with a shoulder at 1466 cm^{-1} [Fig. 4(a), 4(b)] of samples 1–5 arising from the antisymmetric CO stretch^{16,17} is resolved into four, at 1356 , 1370 , 1429 , and 1470 cm^{-1} , in the spectrum of sample 6; these values are very similar to, but shifted from, those of the analogous bands of PbCO_3 . Some of these (for example those at *ca.* 673 – 715 , 837 , 1364 – 1476 , 1679 – 1735 cm^{-1}) correspond to ones at 675 – 700 , 841 , 1356 – 1470 , and 1682 – 1738 cm^{-1} of sample 6. This indicates that PbCO_3 might be formed during the decomposition of $2\text{PbCO}_3 \cdot \text{Pb(OH)}_2$, along with other carbonate oxides, but that it vanishes above 533 K [Fig. 4(e), sample 7].

Fig. 3(a) indicates that a structural transformation takes place between 533 and 613 K , over which range all of the CO_2 is eliminated; this is evident from the band at *ca.* 1052 cm^{-1} (CO symmetric stretch)^{14–16} which continuously decreases in intensity on changing from sample 7 to 11. A strong fluorescent background, possibly associated with structural disorder, accompanies the spectra of these samples. It appears for sample 7 [Fig. 4(e)], increases for 8, passes through a maximum for 9, and decreases for 10 and 11. It appeared only for samples in which quenched mixtures of various lead carbonate oxides had been formed and then decomposed by raising the temperature. Fig. 3(b) shows that above 613 K (sample 11) the elimination of CO_2 is complete and the fluorescent background has vanished; the only Raman bands observed are those attributable to Pb–O modes^{40–43} at 143 – 151 , 287 – 289 , 336 – 341 , 381 – 385 , and 418 – 423 cm^{-1} . Fig 3(b) shows that, beginning with sample 13 (673 K) up to 18 (798 K), a phase transformation³⁶ of PbO takes place.

The Raman spectra of samples 12 and 22 [Figs. 4(g), 4(h)] are characteristic of the tetragonal and orthorhombic phases of PbO, respectively.^{40–43} During this transformation the

symmetry of the elementary cell decreases³⁷ and, consequently, the site symmetries are lowered and the number of Raman-allowed bands is increased. Very weak bands due to lattice modes occur at 73 and 88 cm^{-1} in the spectrum of sample 22.

The very strong band at 142 – 151 cm^{-1} assigned to the PbO symmetric stretch^{40,41} appears in the spectra of samples 6–22. Its shift can therefore be used as an indicator of the structural changes which occur on sample heating. Three phenomena can be observed between 533 and 898 K : the continuous decomposition of lead carbonate oxides takes place in samples 6–10 (533 – 593 K). Sample 11 (613 K) is seen to consist of tetragonal PbO, and it is not until sample 18 (798 K) that the transformation to orthorhombic PbO is complete.

It is concluded that basic lead(II) carbonate decomposes on being heated in static air to give litharge, massicot or mixtures thereof. There is no evidence for Pb_3O_4 [Fig. 4(i), 4(j)] either on thermal decomposition of basic lead(II) carbonate or during the phase transformation of PbO in static air.

X-Ray diffraction. The X-ray diffractograms of samples 1–5 in Fig. 5(a) show only $2\text{PbCO}_3 \cdot \text{Pb(OH)}_2$ and no trace of either plumbonacrite¹¹ or PbCO_3 . Fig. 5(a) shows only one sharp structural change (distinct step) in the decomposition of lead(II) carbonate hydroxide at 483 K (sample 5), above which the water (hydroxide-based) is totally lost. By increasing the temperature the resulting lead carbonate oxides react partially and decompose to give, for samples 6–11, mixtures of general formula $x\text{PbCO}_3 \cdot y\text{PbO}$ in which $x = 1, 2$ or 4 and $y = 1, 2$ or 3 . Table 1 shows that the ratio x/y reduces with increasing temperature in the order $2\text{PbCO}_3 \cdot \text{PbO} > 4\text{PbCO}_3 \cdot 3\text{PbO} > \text{PbCO}_3 \cdot \text{PbO} > \text{PbCO}_3 \cdot 2\text{PbO}$. Since the samples have been quenched, the resulting carbonate oxides may exist as non-stoichiometric and disordered phases.

The X-ray diffractogram of sample 6 shows the characteristic lines of $2\text{PbCO}_3 \cdot \text{PbO}$, $\text{PbCO}_3 \cdot \text{PbO}$ and $4\text{PbCO}_3 \cdot 3\text{PbO}$. There are also weak lines characteristic of PbCO_3 which cannot be seen in the diffractograms of samples 7–11. This demonstrates that PbCO_3 is an intermediate of short lifetime in the decomposition of $2\text{PbCO}_3 \cdot \text{Pb(OH)}_2$. It is remarkable that $4\text{PbCO}_3 \cdot 3\text{PbO}$ does exist between 533 and 568 K (samples 6–8, Table 1). It has previously been reported²⁶ only as a product of synthesis at high pressure and temperature. The formation of $x\text{PbCO}_3 \cdot y\text{PbO}$ structures, which might contain alternate layers of PbCO_3 and PbO, may account for the presence of the strong Raman band at 142 – 151 cm^{-1} (Pb–O symmetric stretch).

The hypothesis of disordered and non-stoichiometric structures is supported by inspecting the FOM of certain carbonate oxides in Table 1. This is a minimum for the sample whose temperature is closest to the equilibrium temperature of a given phase; above this, the FOM values increase, suggesting the development of structural disorder. In Table 1 two different values of FOM are given for some identified lead carbonate oxides whose diffraction lines match those in the X-ray diffraction files for phases of the same formula and structure, but obtained either by decomposition^{24,25} or synthesis.²⁶ However, depending on the preparative procedure, there are small shifts between identical diffraction lines as listed in the files and therefore, by using them as references, different values of FOM will be obtained. In general, the diffractograms of the compounds identified in samples 6–11 (Table 1) match better (*i.e.* FOM smaller) with those given for phases which had been obtained by decomposition.^{24,25}

Table 1 shows that in sample 10 (593 K) $\text{PbCO}_3 \cdot 2\text{PbO}$ exists as a major component, tetragonal PbO begins to appear, and $\text{PbCO}_3 \cdot \text{PbO}$ is not yet totally transformed. The diffractogram of sample 11 [Fig. 5(b)] shows strong lines of tetragonal PbO, accompanied by very weak lines of orthorhombic PbO and $\text{PbCO}_3 \cdot 2\text{PbO}$ which remain as impurities. The tetragonal PbO

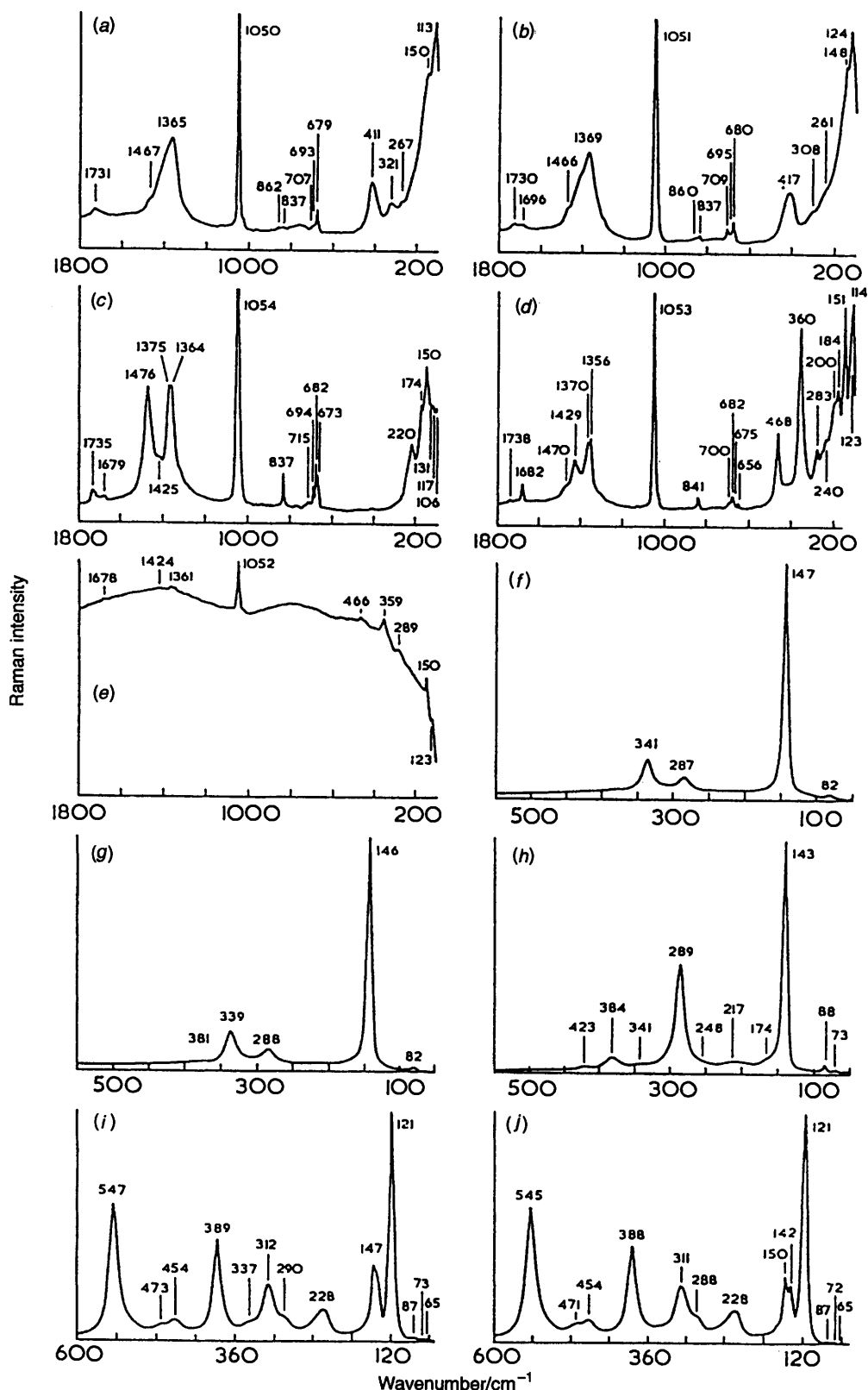


Fig. 4 The FT Raman spectra of several important samples from set 1–22 of reference samples. In this figure only, the ARS macro corrections to the band wavenumbers have been applied (see Experimental section). Samples: (a) $2\text{PbCO}_3 \cdot \text{Pb}(\text{OH})_2$; (b) 5; (c) PbCO_3 ; (d) 6; (e) 7; (f) sample (a) heated in nitrogen at 648 K; (g) 12 (PbO tetragonal); (h) 22 (PbO orthorhombic); (i) sample (a) heated in oxygen at 838 K; (j) Pb_3O_4

is the only component of sample 12, at 643 K. Fig. 5(b) shows that the transformation of tetragonal to orthorhombic PbO ³⁶ occurs continuously over a large range of temperature (about 673–798 K), above which only the orthorhombic phase exists. This may explain the broad endothermic effect detected *via* the DSC curve [Figs. 2(b), 6(b)] over a similar temperature range.

Investigations in flowing nitrogen, in flowing oxygen, and in flowing air

In Fig. 6(a)–6(f) it can be seen that the decomposition of $2\text{PbCO}_3 \cdot \text{Pb}(\text{OH})_2$ occurs either in broadly two steps (flowing nitrogen or flowing air), or in three steps (flowing oxygen), and that it is complete above 618 K, leading in both cases to

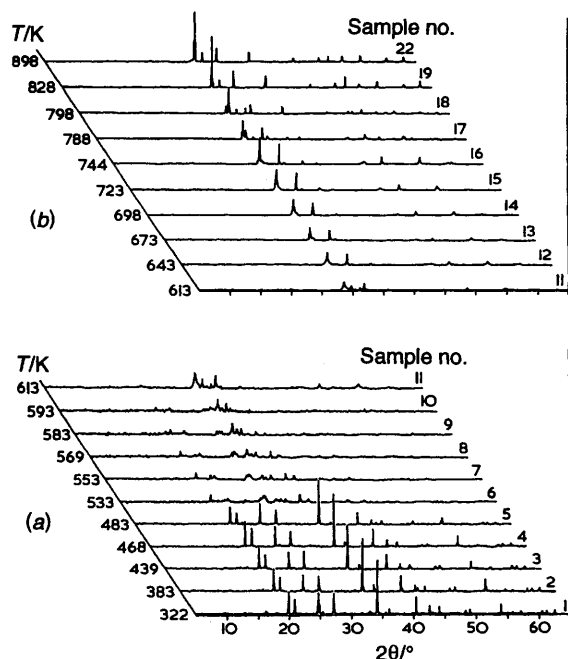


Fig. 5 X-Ray diffractograms of the 22 samples derived from $2\text{PbCO}_3 \cdot \text{Pb}(\text{OH})_2$ on being heated in a tube furnace in static air at increasing temperatures and then quenched at room temperature: (a) samples 1–11; (b) samples 11–22; samples 20 and 21 have not been included since their FT Raman spectra and diffractograms are similar to those of 19 and 22

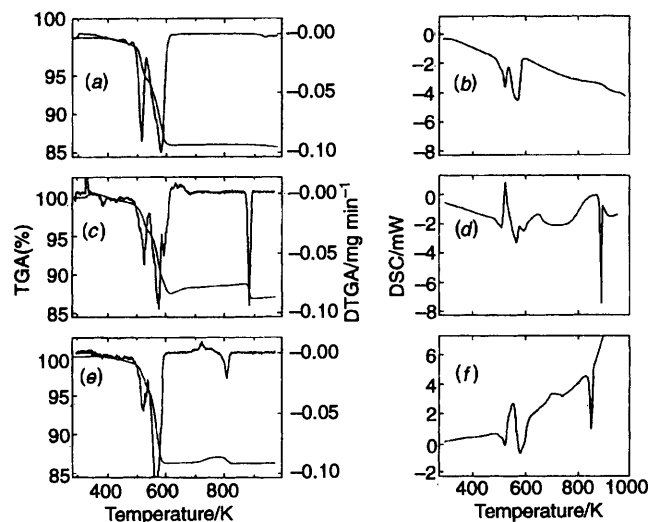


Fig. 6 The TGA and DSC curves of $2\text{PbCO}_3 \cdot \text{Pb}(\text{OH})_2$ heated at 2 K min^{-1} in flowing air in an alumina crucible: (a) TGA/DTGA in nitrogen; (b) DSC in nitrogen; (c) TGA/DTGA in oxygen; (d) DSC in oxygen; (e) TGA/DTGA in flowing air; (f) DSC in flowing air

tetragonal PbO. The TGA/DTGA curves [Fig. 6(a)] show that, above this temperature in an *inert* atmosphere of flowing N_2 , no mass gain is observed. In the range 618–873 K tetragonal PbO transforms slowly into orthorhombic PbO, as is indicated by the broad and weak endothermic peak in the DSC curve [Fig. 6(b)]. This peak is also observed in static air [Fig. 2(a) and 2(b)]. A sample obtained by heating $2\text{PbCO}_3 \cdot \text{Pb}(\text{OH})_2$ in the TGA instrument at 648 K in flowing N_2 gave an FT Raman spectrum [Fig. 4(f)] identical to that prepared in the tube furnace [sample 12, Fig. 4(g)], *i.e.* tetragonal PbO results from basic lead(II) carbonate being heated at 643 K in static air. From the TGA/DTGA data [Fig. 6(c) and 6(e)], which relate to flowing oxygen and flowing air respectively, the observed mass gain can be attributed to the formation of Pb_3O_4 *via* a gas–solid diffusion process. This is accompanied by large and broad

Table 1 The intermediate compounds resulting from the decomposition of basic lead(II) carbonate in static air and identified by X-ray diffraction

Sample number	T/K	Sample composition	FOM ^a	JCPDS number ^b
1–5	294–483	$2\text{PbCO}_3 \cdot \text{Pb}(\text{OH})_2$	0.71	13-131 vs
6	533	$2\text{PbCO}_3 \cdot \text{PbO}$	0.48	18-691 m
		$\text{PbCO}_3 \cdot \text{PbO}$	1.18	17-730 m
			0.45	19-682 s ^c
			0.56	17-729 s
		$4\text{PbCO}_3 \cdot 3\text{PbO}$	0.92	17-732 w
		PbCO_3	1.83	5-417 w
7	553	$2\text{PbCO}_3 \cdot \text{PbO}$	1.34	18-691 w
		$\text{PbCO}_3 \cdot \text{PbO}$	0.87	17-730 w
			1.14	17-729 vs
			0.70	19-682 vs
		$4\text{PbCO}_3 \cdot 3\text{PbO}$	0.44	17-732 s
		$\text{PbCO}_3 \cdot 2\text{PbO}$	1.48	19-681 w
			1.67	17-731 w
8	568	$\text{PbCO}_3 \cdot \text{PbO}$	0.91	19-682 m-s
			0.74	17-729 m-s
		$4\text{PbCO}_3 \cdot 3\text{PbO}$	0.76	7-732 m
		$\text{PbCO}_3 \cdot 2\text{PbO}$	0.92	19-681 s
			0.73	17-731 s
9	583	$\text{PbCO}_3 \cdot \text{PbO}$	1.75	17-729 m
			1.19	19-682 m
		$\text{PbCO}_3 \cdot 2\text{PbO}$	0.57	19-681 s
			0.69	17-731 s
10	593	$\text{PbCO}_3 \cdot \text{PbO}$	1.66	17-729 m-w
			1.07	19-682 m-w
		$\text{PbCO}_3 \cdot 2\text{PbO}$	0.98	19-681 vw
			0.63	17-731 vw
		$\text{PbO}(\text{litharge})$	1.85	5-561 m
11	613	$\text{PbCO}_3 \cdot 2\text{PbO}$	1.34	17-731 vw
		$\text{PbO}(\text{litharge})$	0.73	5-561 vs
		$\text{PbO}(\text{massicot})$	1.39	38-1477 vvw
12	643	$\text{PbO}(\text{litharge})$	0.70	5-561 vvs

^a FOM = Figure of Merit (as given by the EVA program for the Siemens 5000-D diffractometer; FOM = 0 for ideal matching). ^b The characteristic main diffraction lines of the phase identified are s = strong, m = medium, w = weak, v = very. ^c This file has been deleted from JCPDS but its lines match those of the samples studied here better than those given in 17–729.

endothermic effects in the DSC curves [Fig. 6(d) and 6(f)]. The oxidation of tetragonal PbO to Pb_3O_4 takes place in oxygen, in flowing air and in static air provided the sample is maintained for sufficient time (1–2 h) at temperatures above 643 K. However, under normal dynamic TGA conditions in which the sample is held at or above 643 K for a much shorter time tetragonal PbO is the only product. The TGA/DTGA curves [Figs. 6(c) and 6(e)] show that the temperature range for the formation and existence of Pb_3O_4 depends on the experimental conditions, *i.e.* the purge gas, its flow rate, and the reaction time. According to TGA/DTGA and DSC curves, the Pb_3O_4 sharply and strongly endothermically loses oxygen to form orthorhombic PbO over the range 880–898 K in oxygen [Fig. 6(c) and 6(d)] and 785–825 K in air [Fig. 6(e) and 6(f)].

The FT Raman spectrum of a sample of $2\text{PbCO}_3 \cdot \text{Pb}(\text{OH})_2$ heated in a TGA instrument in oxygen at 838 K [Fig. 4(i)] is identical to that of Pb_3O_4 ^{18,19,48} and to that of a reference sample [Fig. 4(j)]. Several weak bands at 65, 72, and 87 cm^{-1} , attributable to lattice modes, can be seen in the spectra of Pb_3O_4 [Fig. 4(i) and 4(j)].

Correlation of observations from X-ray diffraction, thermogravimetry and Raman spectroscopy

In correlating results from X-ray diffraction, thermogravimetry, and Raman spectroscopy the following observations on the decomposition process in static air can be made [Fig. 2(a)]. The first weight loss (0.84%) up to 483 K (samples 1–5) is not

accompanied by structural or compositional changes and is caused by the loss of physically adsorbed water. Analysis by X-ray diffraction of the sample present after the second stage (sample 6, 533 K) showed that it consisted of a mixture of four compounds (Table 1). The formation of these compounds is accompanied by the release of water (hydroxide-based) and CO₂ and an accompanying weight loss of 4.8%; this is confirmed by TGA-mass spectrometry measurements. A small amount of PbCO₃, detected by X-ray diffraction and by Raman spectroscopy, is also formed as an intermediate. It is known that PbCO₃ is a significant intermediate during the decomposition of hydrocerussite in a CO₂ atmosphere.⁴⁹

The carbonatisation of a carbonate oxide by the temporary increased presence of CO₂ is plausible. During further heating up to 553 K PbCO₃ disappears and 4PbCO₃·3PbO appears as the dominant intermediate phase; the latter has not previously been detected under these conditions. The second stage of mass loss reveals in the DTGA curve [Fig. 2(a)] two (and possibly more) processes which amount to an overall mass loss of 8.2% and can be attributed to the progressive decomposition of the intermediate carbonate oxides. The tendency to produce compounds with lower carbonate content accords with the loss of CO₂ as revealed by the X-ray data (2PbCO₃·PbO > 4PbCO₃·3PbO > PbCO₃·PbO > PbCO₃·2PbO). Partial recarbonatisation in the continually changing micro conditions under static air is probable. The formation of tetragonal PbO under these conditions is complete at 643 K (sample 12). The post-decomposition transformation from tetragonal to orthorhombic takes place over the range 673–798 [Fig. 5(b)], giving rise to the broad endothermic peak (635–750 K) in the DSC curve [Fig. 2(b)].

Conclusion

The combined observations suggest that the decomposition of 2PbCO₃·Pb(OH)₂ is more complex than previously thought. In addition, preliminary studies using high-resolution TGA have demonstrated the presence of a number of discrete processes not readily identified by conventional TGA techniques. The decomposition of 2PbCO₃·Pb(OH)₂ depends strongly on the nature of the experimental conditions. In an inert atmosphere [Fig. 7(b)] the DSC curve shows only endothermic processes; in an oxygen-containing atmosphere [Fig. 7(d) and 7(f)] an additional exothermic peak is observed. This can be explained by considering that intermediate carbonate oxides which form in the first stage of decomposition may partially oxidise in an atmosphere rich in oxygen. In the present study it has been possible to isolate two intermediate compounds 4PbCO₃·3PbO and PbCO₃ not previously identified during decomposition in static air under normal atmospheric conditions. These processes also need to be further investigated using *in situ* high-temperature X-ray diffraction techniques and monitoring the decomposition of the sample.

The results also suggest that the composition of the red lead pigment is dependent on the conditions used in its preparation. X-Ray diffraction and thermal analysis data have shown that there are conditions under which Pb₃O₄ is formed either alone or together with tetragonal and/or orthorhombic PbO. Obviously the presence of these different forms and their respective proportions will influence the final colour of the pigment.

Acknowledgements

The authors thank the Leverhulme Trust for a fellowship (to D. A. C.) and both the University of London Intercollegiate Research Service and the Royal Commission for the Exhibition of 1851 for financial support. Professor Armin Reller (University of Hamburg) is thanked for providing the TGA-

mass spectrometric data, Mr. Nick Hawkins (TA Instruments) for providing the high-resolution thermogravimetric data, and Dr. Peter Gibbs and Dr. Stella Casagrande in Felder for their critical reading and evaluation of the manuscript and, in the case of the latter, for generating Figs. 1 and 2.

References

- 1 C. Palachie, H. Berman and C. Frondel, *The System of Mineralogy of J. D. Dana and E. S. Dana*, 7th edn., Wiley, New York, London, 1951, vol. 2, p. 270.
- 2 R. J. Gettens, H. Kuhn and W. T. Chase, in *Artists' Pigments*, ed. A. Roy, Oxford University Press, 1993, vol. 2, pp. 67–81.
- 3 M. Wilcox, *The Wilcox Guide for the Finest Watercolour Paints*, Artwatts, Perth, 1991, p. 270.
- 4 R. J. Gettens and G. L. Stout, *Painting Materials a Short Encyclopaedia*, Dover, New York, 1966, pp. 174–176.
- 5 D. V. Thompson, *The Materials and Techniques of Medieval Paintings*, Dover, New York, 1956, pp. 89–94.
- 6 K. Wehlte, *The Materials and Techniques of Paintings*, Van Nostrand Reinhold, New York, London, 1975, pp. 70–72.
- 7 R. D. Harley, *Artists' Pigments*, Butterworth, London, 1970, pp. 156–161.
- 8 Colour Index, CI77597, Pigment White 1, Society of Dyers and Colourists and American Association of Textile Chemists and Colorists, Bradford and London, 3rd edn., 1971, vol. 4, p. 4676.
- 9 R. G. Wyckoff, *Crystal Structures*, 2nd edn., Wiley-Interscience, New York, 1965, vol. 2, pp. 367, 479.
- 10 J. M. Cowley, *Acta Crystallogr.*, 1956, **9**, 391.
- 11 J. K. Olby, *J. Inorg. Nucl. Chem.*, 1966, **28**, 2507.
- 12 H. E. Swanson and R. K. Fuyat, *Nat. Bur. Stand. (U.S.)*, 1953, *Circ.* 539 II, 56; II, 30.
- 13 G. Chevrier, G. Giester, G. Heger, D. Jarosch, M. Wildner and J. Zemann, *Z. Kristallogr.*, 1992, **199**, 67.
- 14 W. P. Griffith, *J. Chem. Soc. A*, 1970, 286.
- 15 R. Durman, U. A. Jayasooriya and S. F. A. Kettle, *J. Chem. Soc., Chem. Commun.*, 1985, 916.
- 16 W. P. Griffith, in *Advances in Spectroscopy*, eds R. J. H. Clark and R. E. Hester, Wiley, Chichester, 1987, vol. 14, p. 138.
- 17 E. E. Coleyshaw and W. P. Griffith, *Spectrochim. Acta, Part A*, 1994, **50**, 1909.
- 18 S. P. Best, R. J. H. Clark and R. Withnall, *Endeavour*, 1992, **16**, 66.
- 19 S. P. Best, R. J. H. Clark, R. Withnall and M. A. M. Daniels, *Chem. Br.*, 1993, **29**, 118.
- 20 T. L. Webb and J. E. Kruger, in *Differential Thermal Analysis*, ed. R. C. McKenzie, Academic Press, London, 1970, pp. 302–341.
- 21 D. N. Todor, *Thermal Analysis of Minerals*, Abacus Press, Tunbridge, 1976, p. 169.
- 22 C. W. Beck, *Am. Mineral.*, 1950, **36**, 985.
- 23 S. St. J. Warne and P. Bayliss, *Am. Mineral.*, 1962, **47**, 1011.
- 24 G. Pannetier, S. Fenistein and G. D. Mariadassou, *Bull. Soc. Chim. Fr.*, 1964, 701.
- 25 G. Pannetier, S. Fenistein and L. Davignon, *Bull. Soc. Chim. Fr.*, 1965, 109.
- 26 D. Grissafe and W. B. White, *Am. Mineral.*, 1964, **49**, 1184.
- 27 G. C. Vezzoli and S. Krasner, *High Temp.-High Pressures*, 1983, **15**, 27.
- 28 G. C. Vezzoli and S. Krasner, *High Temp.-High Pressures*, 1983, **15**, 41.
- 29 E. S. Larsen, *Am. Mineral.*, 1917, **2**, 18.
- 30 M. I. Kay, *Acta Crystallogr.*, 1961, **14**, 80.
- 31 J. Leciejewicz, *Acta Crystallogr.*, 1961, **14**, 66.
- 32 G. R. Levi, *Nuova Cimento*, 1924, **1**, 335.
- 33 F. Halla and F. Pawlek, *Z. Phys. Chem.*, 1927, **128**, 49.
- 34 R. G. Wyckoff, *Crystal Structures*, 2nd edn., Wiley-Interscience, New York, 1963, vol. 1, pp. 134, 137.
- 35 H. McMurdie, *Powder Diffraction*, 1987, **2**, 46.
- 36 W. B. White, F. Dacheille and R. Roy, *J. Ceram. Soc.*, 1961, **44**, 170.
- 37 R. Soderquist and B. Dickens, *J. Phys. Chem. Solids*, 1967, **28**, 823.
- 38 B. Dickens, *J. Inorg. Nucl. Chem.*, 1965, **27**, 1495.
- 39 B. Dickens, *J. Inorg. Nucl. Chem.*, 1965, **27**, 1503.
- 40 J. D. Donaldson, M. T. Donoghue and S. D. Ross, *Spectrochim. Acta, Part A*, 1974, **30**, 1967.
- 41 D. M. Adams and D. C. Stevens, *J. Chem. Soc., Dalton Trans.*, 1977, 1096.
- 42 K. R. Bullock, G. M. Trischan and R. G. Burrow, *J. Electrochem. Soc., Electrochem. Sci. Technol.*, 1983, **130**, 1283.

- 43 G. L. J. Trettenhahn, G. E. Nauer and A. Neckel, *Vibr. Spectrosc.*, 1993, **5**, 85.
- 44 E. W. Fitzhugh, in *Artists' Pigments*, ed. R. L. Feller, Cambridge University Press, 1986, vol. 1, pp. 109–139.
- 45 G. L. Clark and R. Rowan, *J. Am. Chem. Soc.*, 1941, **63**, 1302.
- 46 I. J. Lin and S. Niedwiedz, *J. Am. Ceram. Soc.*, 1973, **56**, 62.
- 47 J. M. Criado, F. Gonzales, M. Gonzales and C. Real, *J. Mater. Sci.*, 1982, **17**, 2056.
- 48 J. P. Vigoroux, E. Husson, G. Galvarin and N. Q. Dao, *Spectrochim. Acta, Part A*, 1982, **38**, 393.
- 49 J. Yamaguchi, Y. Sawada, O. Sakurai, K. Uematsu, N. Mizutani and M. Kato, *Thermochim. Acta*, 1980, **37**, 79.

Received 11th March 1996; Paper 6/01691J